Available online at www.sciencedirect.com
ScienceDirect
Trans. Nonferrous Met. Soc. China 35(2025) 990−999
Transactions of Nonferrous Metals Society of China
www.tnmsc.cn

Competitive behaviors between tungsten and iron in TBP−HCl−H_2O extraction system

Li-qin DENG[1], Xu-heng LIU[1], Xing-yu CHEN[1], Jiang-tao LI[1,2], Li-hua HE[1], Feng-long SUN[1,2], Zhong-wei ZHAO[1,2]

1. School of Metallurgy and Environment, Central South University, Changsha 410083, China;
2. Key Laboratory of Hunan Province for Metallurgy and Material Processing of Rare Metals, Central South University, Changsha 410083, China

Received 5 July 2023; accepted 21 March 2024

Abstract: The distribution and competitive behaviors of phosphotungstic acid and ferric chloride in the TBP–HCl–H_2O system were investigated by controlling the extractant concentration and the solution environment. The results revealed that phosphotungstic acid exhibited a strong affinity for TBP with decreasing TBP concentration. Higher acidity significantly improved the W extraction efficiency with TBP, and the lower Cl^- concentration reduced the extraction efficiency of Fe. As the organic phase approached saturation point, phosphotungstic acid competitively displaced Fe to combine with TBP. The hydrogen bond structure (P═O·HO—P—W—O) between phosphotungstic acid and TBP was characterized by FT-IR, and the salting-out effect induced by $FeCl_3$ was elucidated. In summary, high acidity is beneficial for exhaustive extraction of W, and an effective W/Fe separation can be achieved by reducing the concentrations of TBP and Cl^-.

Key words: solvent extraction; tri-butyl phosphate; tungsten/iron separation; distribution equilibrium; competitive behavior

1 Introduction

Tungsten and its compounds are vital components in advanced manufacturing industries, such as machinery, electronics, aerospace, and defense [1−5]. Primary mineral sources of tungsten include scheelite ($CaWO_4$) and wolframite [$(Fe,Mn)WO_4$] [6]. However, extensive mining activities have led to the depletion of high-quality single-component minerals. Complex low-grade tungsten concentrate has been became the main raw material, which includes the increased content of impurities [7,8]. Consequently, there are increased pressures on the mineral decomposition and the subsequent purification processes.

Classical hydrometallurgy processes of tungsten concentrate involve soda autoclaving and caustic soda autoclaving methods, and tungsten is converted into soluble sodium tungstate [9,10]. Owing to the heightened stringency of environmental protection measures, the traditional processes have been limited tightly [10]. In this case, the acidic process for extracting tungsten ore has emerged as a prominent industrial method owing to its superior cleanliness and efficiency [11,12]. However, numerous iron impurities are introduced into the phosphotungstic acid leachate during a low-grade concentrate decomposition process. The hydrolysis of Fe(III) hinders the subsequent purification step, and its strong adsorption results in the loss of tungsten. Therefore, the effective separation of tungsten and iron in acidic system is challenging.

The solvent extraction method is widely used in metallurgical separation process. Tri-butyl phosphate

Corresponding author: Xu-heng LIU, Tel: +86-731-88830476, E-mail: liuxuheng@csu.edu.cn
DOI: https://doi.org/10.1016/S1003-6326(24)66729-4

(TBP) has been extensively studied for extracting phosphotungstic acid and iron [13−15]. In the acidic system, TBP exhibits a strong extraction ability for phosphotungstic acid ($H_3PW_{12}O_{40}$) to form the complexes through hydrogen bonding interaction. The distribution ratio of W is influenced by the H^+ concentration in the aqueous phase and the free-TBP concentration in the organic phase [16,17]. Generally, TBP does not extract cations such as Fe(II) and Fe(III). However, Cl^- can combine with Fe(III) to form a complex anion, which easily binds with TBP in organic phase [18−21]. The speciation of both phosphotungstic acid and ferric complex anion are sensitive to pH value, and various species hold different affinities to TBP in the extraction mechanism. Thus, it is vital to elucidate the relationship between variable parameters and reaction mechanisms in this solvent extraction system. Owing to the variability of the ion concentration and solution environment in industrial practice, a trial-and-error approach for adjusting parameters is ineffective. Therefore, elucidating the distribution pattern and competitive mechanisms of tungsten and iron in the TBP−HCl−H_2O system is crucial.

This study extensively explored the variable parameter effects on the distribution equilibrium and the separation of W/Fe. The competitive behavior between W and Fe in the solvent extraction system was examined under the experimental conditions related to the maximum loading process. The respective binding forms of W and Fe with organic extractants were characterized by Fourier-transform infrared spectroscopy (FT-IR). The findings of this study elucidated the distribution and competitive behavior of W and Fe, and provided effective theoretical guidance for designing extraction and separation processes.

2 Experimental

2.1 Materials and reagents

The research subjects were prepared by dissolving $H_3PW_{12}O_{40}\cdot xH_2O$ (AR, Chron Chemicals Reagent, Co., Ltd.) and $FeCl_3\cdot 6H_2O$ (AR, Sinopharm Chemical Reagent Co., Ltd.) in a certain concentration hydrochloric acid (AR, Chron Chemicals Reagent, Co., Ltd.) solution. Sulfuric acid (AR, Chron Chemicals Reagent, Co., Ltd.) and NaCl (AR, Sinopharm Chemical Reagent Co., Ltd.) were analytical grade, and the deionized water with a resistivity of 18.2 MΩ/cm was used in the experiments. The organic phase consisted of the required amount of tri-butyl phosphate (TBP) (Hunan Huihong Reagent, Co., Ltd.) and the diluent (Sulfonated kerosene, density = 786 kg/m^3, boiling range = 200−250 °C, supplied by Weng Jiang Reagent, Co., Ltd.).

2.2 Experimental operation

40 mL acidic simulation solution and the organic phase were mixed in a 125 mL separatory funnel, and then the funnel was shaken on the mechanical shaker at a temperature of (25±2) °C. The reaction time of 60 min was controlled to ensure that the extraction reached equilibrium. Afterwards, the loading organic phase and equilibrium aqueous phase were separated, and 1 mL raffinate was collected for analysis. The distribution coefficient (D) and separation factor (β) were calculated by Eqs. (1) and (2), respectively:

$$D=\frac{[\mathrm{M}]_{\mathrm{org}}}{[\mathrm{M}]_{\mathrm{aq}}}=\frac{([\mathrm{M}]_{\mathrm{ini}}-[\mathrm{M}]_{\mathrm{fin}})\cdot\frac{V_{\mathrm{O}}}{V_{\mathrm{A}}}}{[\mathrm{M}]_{\mathrm{fin}}} \tag{1}$$

$$\beta_{i/j}=D_i/D_j \tag{2}$$

where $[M]_{org}$ and $[M]_{aq}$ represent the equilibrium concentrations of metal ions in the organic phase and aqueous phase, respectively; $[M]_{ini}$ and $[M]_{fin}$ represent the initial and final concentrations of metal ions in the aqueous phase, respectively; V_O and V_A are the volumes of the organic and aqueous phases, respectively; D_i and D_j are the distribution coefficient of metal ions in the extraction system, respectively.

2.3 Analysis and characterization

ICP-OES (iCAP 7200 Radial, Thermo Fisher Scientific, USA) was used to measure the concentrations of metal ion in aqueous phase. And the organic phase was characterized by Fourier Transform Infrared Spectroscopy (FT-IR, Thermo Fisher/Nicolet iS50, USA) in the wavenumber range of 4000−400 cm^{-1}.

2.4 Establishment of distribution research method

In this research, the logarithm distribution plots of the species versus system parameters were constructed to investigate the distribution behaviors and interrelationship of tungsten and iron. The

relationships between the variables and experimental data were developed based on theoretical reaction formulas, and the assumptions were taken [22−24]: (1) the variable concentration of species in the aqueous phase does not affect the activity coefficient and ionic strength; (2) only a single tungsten or iron form is considered to exist in organic phase. When the initial pH of the aqueous phase was controlled strictly, the presence of other metallic species were deemed to be extremely small, which could be negligible [25,26].

3 Results and discussion

3.1 Effect of TBP concentration on distribution of W and Fe

According to the assumptions outlined in Section 2.4, the extraction process considered a single metallic species (phosphotungstic acid or ferric chloride). Thus, the reactions between the metallic species and TBP are represented in Eqs. (3) and (4) [27−29].

$$2H^+_{(aq)}+HPW_{12}O^{2-}_{40\,(aq)}+n\overline{TBP}_{(org)}=\overline{H^+\cdot n\mathrm{TBP}\cdot H_2PW_{12}O^-_{40\,(org)}} \tag{3}$$

$$H^+_{(aq)}+Fe^{3+}_{(aq)}+4Cl^-_{(aq)}+n\overline{TBP}_{(org)}=\overline{H^+\cdot n\mathrm{TBP}\cdot FeCl^-_{4\,(org)}} \tag{4}$$

$$K_1=\frac{\left[a\overline{H^+\cdot n\mathrm{TBP}\cdot H_2PW_{12}O^-_{40\,(org)}}\right]}{[aH^+_{(aq)}]^2\cdot[aHPW_{12}O^{2-}_{40\,(aq)}]\cdot[a\overline{TBP}_{(org)}]^n}=\frac{\left[\overline{H^+\cdot n\mathrm{TBP}\cdot H_2PW_{12}O^-_{40\,(org)}}\right]}{[H^+_{(aq)}]^2\cdot[HPW_{12}O^{2-}_{40\,(aq)}]\cdot[\overline{TBP}_{(org)}]^n}\cdot Q_1 \tag{5}$$

$$K_2=\frac{\left[a\overline{H^+\cdot n\mathrm{TBP}\cdot FeCl^-_{4\,(org)}}\right]}{[aH^+_{(aq)}]\cdot[aFe^{3+}_{(aq)}]\cdot[aCl^-_{(aq)}]^4\cdot[a\overline{TBP}_{(org)}]^n}=\frac{\left[\overline{H^+\cdot n\mathrm{TBP}\cdot FeCl^-_{4\,(org)}}\right]}{[H^+_{(aq)}]\cdot[Fe^{3+}_{(aq)}]\cdot[Cl^-_{(aq)}]^4\cdot[\overline{TBP}_{(org)}]^n}\cdot Q_2 \tag{6}$$

The extraction processes of phosphotungstic acid and iron were described by the thermodynamic equilibrium constant (K_1 and K_2), as expressed in Eqs. (5) and (6). The activity coefficient was assumed as constant; Q_1 and Q_2 represent the quotient of the activity coefficients of the components in the organic and aqueous phases, respectively. The distribution coefficient (D) was defined as the concentration of the metal ion in the organic phase to that in the aqueous phase. The derivation process of logarithm ($\lg D$) was described as Eqs. (7)−(10).

$$D_1=\frac{\left[\overline{H^+\cdot n\mathrm{TBP}\cdot H_2PW_{12}O^-_{40\,(org)}}\right]}{\left[HPW_{12}O^{2-}_{40\,(aq)}\right]}=K_1\cdot\left[\overline{TBP}_{(org)}\right]^n\cdot[H^+_{(aq)}]^2\cdot\frac{1}{Q_1} \tag{7}$$

$$D_2=\frac{\left[\overline{H^+\cdot n\mathrm{TBP}\cdot FeCl^-_{4\,(org)}}\right]}{\left[Fe^{3+}_{(aq)}\right]}=K_2\cdot\left[\overline{TBP}_{(org)}\right]^n\cdot[H^+_{(aq)}]\cdot[Cl^-_{(aq)}]^4\cdot\frac{1}{Q_2} \tag{8}$$

$$\lg D_1=\lg\frac{K_1}{Q_1}+n\lg\left[\overline{TBP}_{(org)}\right]+2\lg[H^+_{(aq)}] \tag{9}$$

$$\lg D_2=\lg\frac{K_2}{Q_2}+n\lg\left[\overline{TBP}_{(org)}\right]+\lg[H^+_{(aq)}]+4\lg[Cl^-_{(aq)}] \tag{10}$$

The distribution patterns of tungsten and iron in the solvent extraction process were initially determined by plotting the distribution of the species against the of variables, as shown in Fig. 1. The initial concentration conditions of the aqueous phase were maintained at 4 mol/L of HCl, 0.167 mol/L of W and 0.5 mol/L of Fe. TBP concentration was controlled from 0.5 to 3.0 mol/L in the organic phase.

Figure 1 shows a plot of lg D versus lg [TBP] based on Eqs. (9) and (10). This plot elucidated the distribution pattern of tungsten and iron in the HCl−TBP−H_2O system. The trend observed in the two lines represented the logarithmic distribution of tungsten and iron based on the function of lg [TBP]. The slopes of these lines indicated the molar ratios relationship between the extracted species and TBP, showing a molar ratio of TBP:W=1.59:1 and TBP:Fe=3.56:1 in the loaded organic phase. Fe established a competitive relationship with W, and required a higher number of TBP molecules to form complexes. At a lower TBP concentration of 0.5 mol/L, the lg D of W is 2.51 and the lg D of Fe is −0.34. Both the distribution coefficients of W and Fe displays an upward trend with increased TBP concentration. The lg D of Fe rapidly increased as the TBP concentration increased, indicating an enhancement in the extraction efficiency of Fe when a sufficient number of free-TBP molecules were available.

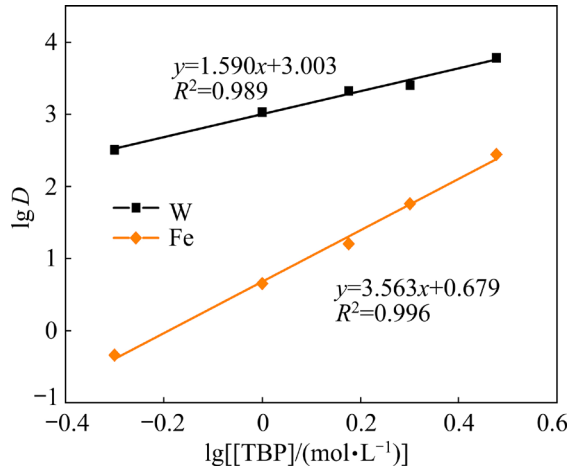

Fig. 1 Influence of TBP concentration on W and Fe distribution (Aqueous phase: $[H^+]$=4 mol/L, $[Cl^-]$=4 mol/L, [W]=0.167 mol/L, and [Fe(III)]=0.5 mol/L; Organic phase: [TBP]=0.5−3.0 mol/L, and T=(25±2) °C)

Figure 2 illustrates the separation factor between tungsten (W) and iron (Fe). As the TBP concentration increased from 0.5 to 1.5 mol/L, the W concentration of the equilibrium aqueous phase decreased from 2.27×10^{-2} to 3.13×10^{-3} g/L, and the concentration of Fe decreased from 18.85 to 0.04 g/L after extraction. This indicates that a TBP concentration of 0.5 mol/L was sufficient for the effective extraction of W. Phosphotungstic acid exhibited a stronger affinity for TBP when free-TBP molecules were scarce, and TBP preferentially formed an extractive complex with phosphotungstic acid. Therefore, the effective separation between W and Fe can be achieved by controlling a lower TBP concentration.

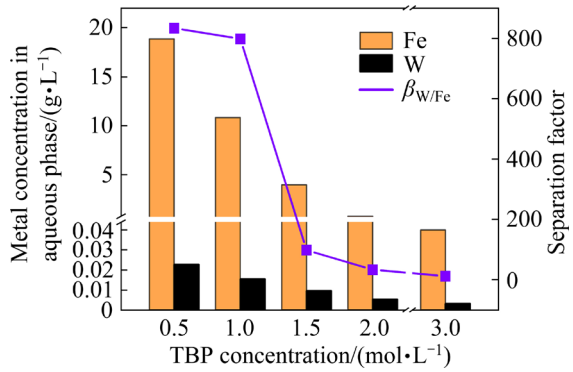

Fig. 2 Metal concentration in equilibrium aqueous phase and separation factor under various TBP concentrations (Aqueous phase: $[H^+]$=4 mol/L, $[Cl^-]$=4 mol/L, [W]=0.167 mol/L, and [Fe(III)]=0.5 mol/L; Organic phase: [TBP]=0.5−3.0 mol/L, and T=(25±2) °C)

3.2 Effect of H^+ and Cl^- concentration on distribution of W and Fe

The speciation of both phosphotungstic acid and iron in the aqueous phase is influenced by pH. SMITH and PAIRICK [14] proposed that phosphotungstic acid solely exists as the Keggin-type $H_3PW_{12}O_{40}$ at pH<0.76. When the pH is higher than 0.76, phosphotungstic acid converts to the Dawson-type $H_6P_2W_{18}O_{62}$ and Keggin-type $H_7PW_{11}O_{39}$ in the solution. However, the forms of Dawson-type $H_6P_2W_{18}O_{62}$ and Keggin-type $H_7PW_{11}O_{39}$ exhibit significantly lower extraction efficiency with TBP than the Keggin-type $H_3PW_{12}O_{40}$. Fe(III) gradually transforms into the complex anion in HCl medium. Under different Cl^- concentration conditions, the equilibrium reactions between Fe(III) and Cl^- involve the Reactions (11)−(14). At higher Cl^- concentrations, $FeCl_4^-$ is the main complex form in solution [11].

$$Fe^{3+}+Cl^- \rightleftharpoons FeCl^{2+} \quad (11)$$

$$FeCl^{2+}+Cl^- \rightleftharpoons FeCl_2^+ \quad (12)$$

$$FeCl_2^++Cl^- \rightleftharpoons FeCl_3 \quad (13)$$

$$FeCl_3+Cl^- \rightleftharpoons FeCl_4^- \quad (14)$$

According to Eqs. (9) and (10), the distribution coefficient of W is greatly influenced by H^+ concentration, and the distribution coefficient of Fe is affected by both H^+ concentration and Cl^- concentration. The individual effects of H^+ and Cl^- on the distribution pattern were investigated, as shown in Figs. 3 and 4. The H^+ concentration was

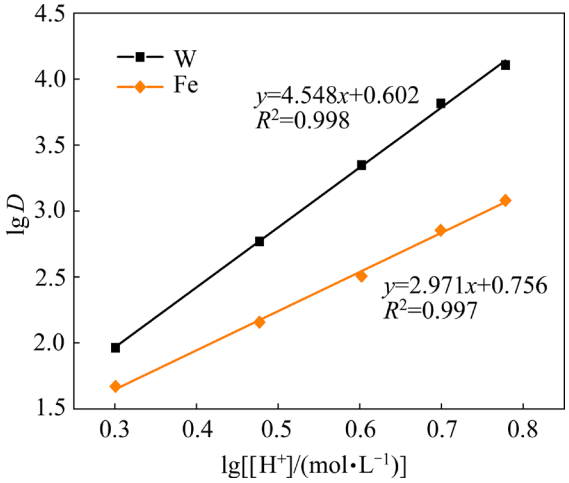

Fig. 3 Influence of H^+ concentration on W and Fe distribution (Aqueous phase: $[H^+]$=2.0−6.0 mol/L, $[Cl^-]$=4.0 mol/L, [W]=0.167 mol/L, and [Fe(III)]=0.5 mol/L; Organic phase: [TBP]=2.5 mol/L, and T=(25±2) °C)

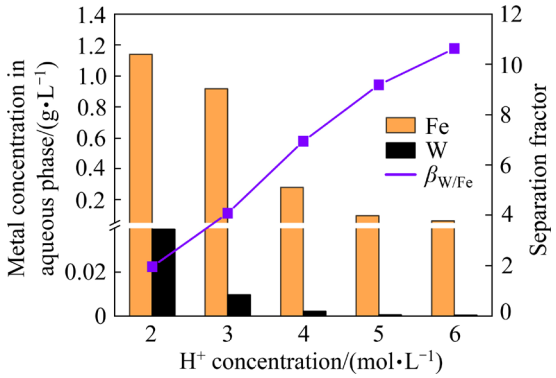

Fig. 4 Metal concentration in equilibrium aqueous phase and separation factor under various H^+ concentrations (Aqueous phase: $[H^+]$=2.0−6.0 mol/L, $[Cl^-]$=4.0 mol/L, [W]=0.167 mol/L, and [Fe(III)]= 0.5 mol/L; Organic phase: [TBP]=2.5 mol/L, and T=(25±2) °C)

adjusted through the addition of H_2SO_4, and the Cl^- concentration was adjusted by adding NaCl (neither SO_4^{2-} nor Na^+ affects the present form of W and Fe in the solution).

Figure 3 shows a plot of lg D versus lg $[H^+]$. According to Eqs. (9) and (10), the formation of $[H^+]^2 \cdot [HPW_{12}O_{40}^{2-}] \cdot [TBP]^n$ requires more free-H^+, so increased acidity is helpful for the formation of extraction complex. The steeper slope of the line of W indicates that increased acidity is more advantageous in facilitating the migration of W to the organic phase. As the concentration of H^+ increased from 2 to 6 mol/L, the concentration of W in the equilibrium aqueous phase decreased from 3.95×10^{-2} to 5.40×10^{-4} g/L (Fig. 4), revealing that increasing the H^+ concentration in the initial aqueous phase effectively reduced the residual W concentration in the equilibrium aqueous phase. Therefore, increasing the H^+ concentration of the aqueous phase promoted the effective extraction of W in this extraction system.

Figure 5 shows a plot of lg D versus lg $[Cl^-]$. As the Cl^- concentration increased, the lg D of Fe also significantly increased. Because the form of $FeCl_4^-$ is the most easily extracted species by TBP, a higher Cl^- concentration is beneficial for the extraction efficiency of Fe. As the Cl^- concentration increased from 1 to 3 mol/L, the concentration of Fe in the equilibrium aqueous phase rapidly decreased from 5.77 to 0.14 g/L, and the separation factor $\beta_{W/Fe}$ decreased from 184.06 to 4.34 (Fig. 6). Therefore, the Cl^- concentration is a critical factor in the complex formation between Fe and TBP, and a lower Cl^- concentration is beneficial for reducing the extraction efficiency of Fe.

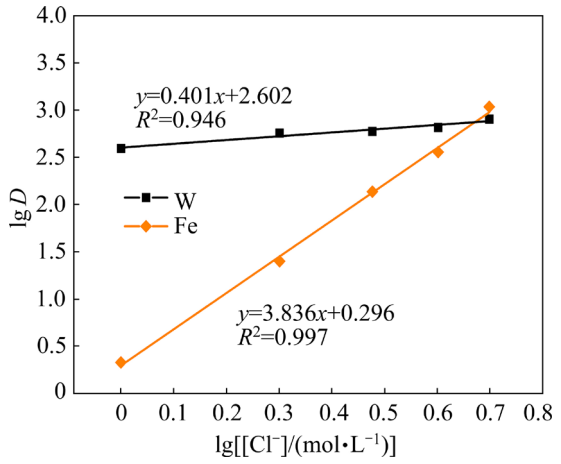

Fig. 5 Influence of Cl^- concentration on W and Fe distribution (Aqueous phase: $[Cl^-]$=1.0−5.0 mol/L, $[H^+]$= 4.0 mol/L, [W]=0.167 mol/L, and [Fe(III)]=0.5 mol/L; Organic phase: [TBP]=2.0 mol/L, and T=(25±2) °C)

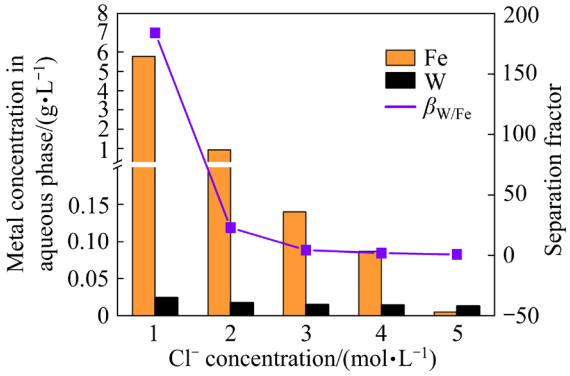

Fig. 6 Metal concentration in equilibrium aqueous phase and separation factor under various Cl^- concentrations (Aqueous phase: $[Cl^-]$=1.0−5.0 mol/L, $[H^+]$=4.0 mol/L, [W]=0.167 mol/L, and [Fe(III)]=0.5 mol/L; Organic phase: [TBP]=2.0 mol/L, and T=(25±2) °C)

Generally, the extraction process of W should not be influenced by Cl^-. However, Figs. 5 and 6 demonstrate a slight increase in the extraction efficiency of W with the increase of Cl^- concentration. The distribution equilibrium of W may be affected by the salting-out effect of $FeCl_3$.

3.3 Impact of $FeCl_3$ on thermal effect and reaction equilibrium

The impact of various Fe(III) concentrations on the distribution of W was investigated. According to the distribution coefficient (D) of the phosphotungstic acid (Eq. (7)), the natural

logarithm was applied to both sides of Eq. (7) to obtain Eq. (15).

$$\ln D=-\frac{\Delta H}{RT}+n\ln\left[\overline{\mathrm{TBP}}_{(\mathrm{org})}\right]+2\ln[\mathrm{H}^{+}_{(\mathrm{aq})}]+C \quad (15)$$

where ΔH is the enthalpy change, and C is a constant.

In a certain temperature range, the influence of temperature on the logarithm term of H^+ and TBP can be disregarded. The equation can be simplified as Eq. (16):

$$\ln D=-\frac{\Delta H}{RT}+C' \quad (16)$$

where C' is a constant.

According to Eq. (16), $\ln D$ versus $1/T$ is presented in Fig. 7. The extraction conditions were controlled as 3 mol/L TBP, t=60 min, V_O/V_A=1/1, and the temperature range of 20 to 60 °C.

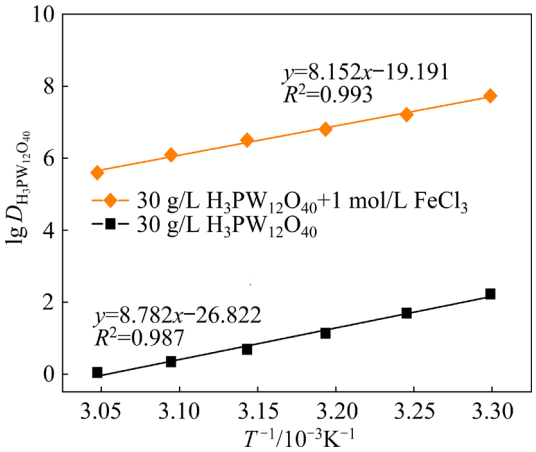

Fig. 7 Effect of $FeCl_3$ concentration in aqueous solution on $\ln D$–T^{-1} relationship (Aqueous phase: [HCl]= 4.0 mol/L, [$H_3PW_{12}O_{40}$]=30 g/L, and [$FeCl_3$]=1.0 mol/L; Organic phase: [TBP]=3.0 mol/L, and T=20−60 °C)

The results show a linear correlation between $\ln D$ of $H_3PW_{12}O_{40}$ and the T^{-1} as the extraction equilibrium is reached. Owing to the salting-out effect of strong electrolytes, the incorporation of $FeCl_3$ led to an increase in the $\ln D$ of $H_3PW_{12}O_{40}$. According to the slope value in Fig. 7, the enthalpy of the extraction reaction can be calculated. ΔH_1 represented the enthalpy of the extraction reaction between phosphotungstic acid and TBP when the $FeCl_3$ concentration was 1.0 mol/L, and ΔH_2 represented the enthalpy of the extraction reaction between phosphotungstic acid and TBP.

ΔH_1=(−8.152×8.314) kJ/mol=−67.8 kJ/mol

ΔH_2=(−8.782×8.314) kJ/mol=−73.0 kJ/mol

The enthalpy values (ΔH_1 and ΔH_2) were calculated as −67.8 and −73.0 kJ/mol, respectively. The extraction reaction between TBP and $H_3PW_{12}O_{40}$ was exothermic, and the $FeCl_3$ component in the aqueous phase mitigated the thermal effect of the reaction.

According to Eq. (9), the extraction efficiency and distribution coefficient of W were investigated at different concentrations of $FeCl_3$ in the aqueous phase. The V_O/V_A ratio, initial W concentration in the aqueous phase, and extraction temperature were held constant. The relationship between the lg D of W and lg [TBP] under various initial $FeCl_3$ concentrations in the aqueous phase is illustrated in Fig. 8.

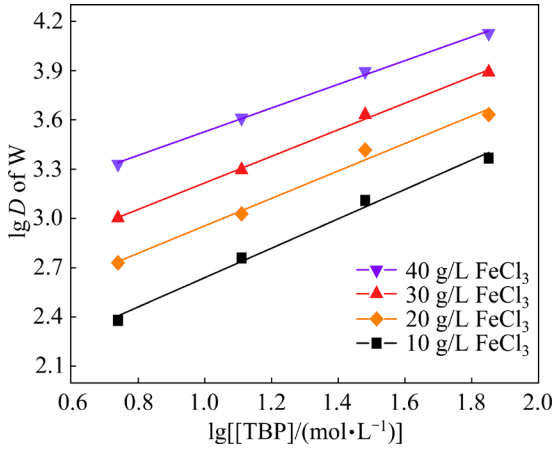

Fig. 8 Variation curves of lg$D$–lg[TBP] under different $FeCl_3$ concentrations (Aqueous phase: [HCl]=4.0 mol/L, [$H_3PW_{12}O_{40}$]=30 g/L, and [$FeCl_3$]= 10−40 g/L; Organic phase: [TBP]=20−50 vol.%, and T=(25±2) °C)

Four straight lines represented the relationship between the lg D of W and lg [TBP]. The distribution coefficient of W increased with increasing TBP concentration, and an increasing concentration of $FeCl_3$ in the aqueous phase enhanced the extraction efficiency of W. The molar ratio n of extracted species to TBP can be calculated from the slope value. The n value and the specific extraction complex $\overline{\mathrm{H_3PW_{12}O_{40}}\cdot n\mathrm{TBP}}$ are shown in Table 1. As the concentration of $FeCl_3$ increased in the range of 10−40 g/L, the formation of extraction complexes $\overline{\mathrm{H_3PW_{12}O_{40}}\cdot(0.72\sim0.89)\mathrm{TBP}}$ became evident. Thus, the phosphotungstic acid could form complexes with fewer TBP molecule as the $FeCl_3$ concentration increased. Figure 9 shows

the effect of $FeCl_3$ concentration on the extraction efficiency of W. When the TBP content was 20 vol.%, the extraction efficiency of W increased from 99.53% to 99.97% as the $FeCl_3$ concentration in the aqueous phase increased from 20 to 50 g/L. The composition of the extraction complex between $H_3PW_{12}O_{40}$ and TBP was slightly influenced by the $FeCl_3$ concentration. The presence of $FeCl_3$ in the aqueous phase was beneficial to the complex extraction reaction of $H_3PW_{12}O_{40}$.

Table 1 Apparent extracted complex under various $FeCl_3$ concentrations in aqueous solution

ρ_{FeCl_3} / (g·L^{-1})	n	R^2	Molecular formula of apparent extracted complex
10	0.89	0.993	$H_3PW_{12}O_{40}$·0.89TBP
20	0.84	0.989	$H_3PW_{12}O_{40}$·0.84TBP
30	0.81	0.998	$H_3PW_{12}O_{40}$·0.81TBP
40	0.72	0.998	$H_3PW_{12}O_{40}$·0.72TBP

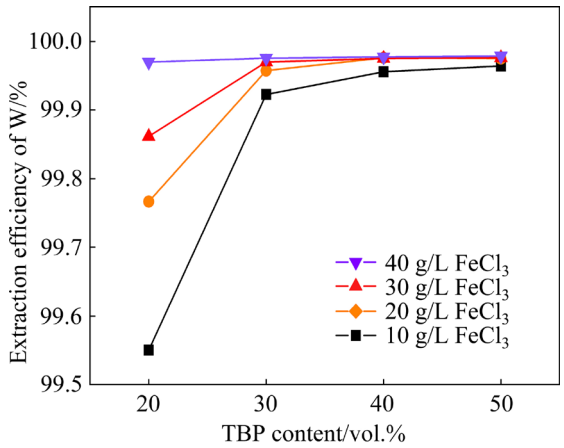

Fig. 9 Effect of $FeCl_3$ concentration on extraction efficiency of W (Aqueous phase: [HCl]=4.0 mol/L, $[H_3PW_{12}O_{40}]$=30 g/L, and $[FeCl_3]$=10−40 g/L; Organic phase: [TBP]=20−50 vol.%, and T=(25±2) °C)

3.4 Saturated load of extraction system and characterization of extracted complex

The equilibrium state of W and Fe in the TBP extraction system was investigated under higher load condition. The saturation of the organic phase was prepared by repeatedly mixing the organic phase with a fresh aqueous phase, and the changes in the concentration of elements in the loaded organic phase are shown in Fig. 10.

In the continuous contact extraction process, Fe preferentially reached saturation at 411.64 g/L in the loaded organic phase (Fig. 10). After 16 successive contacts with the fresh aqueous phase, the extraction system achieved a maximum saturation capacity of W (580.23 g/L). The ratio curve of the W/Fe concentration clearly indicated that the binding of phosphotungstic acid and TBP takes precedence. The extraction between Fe and additional free-TBP molecules causes a decline in the W/Fe concentration ratio in the organic phase. After 12 contact cycles with the fresh aqueous phase, the competition effect of phosphotungstic acid induced the stripping of Fe from the organic phase, and a rapid increase of the W/Fe concentration ratio was obvious. Therefore, the complex $\overline{H_3PW_{12}O_{40}\cdot n\text{TBP}}$ was more stability.

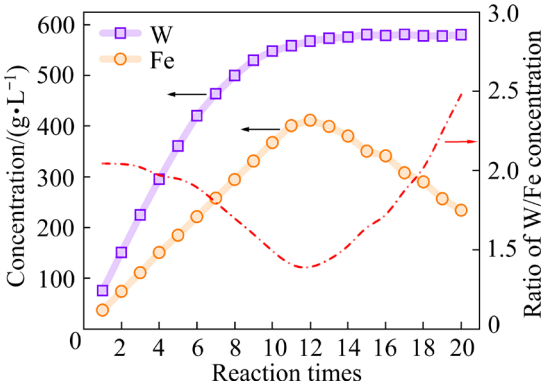

Fig. 10 Variation and ratio of element concentration in loaded organic phase with contact reaction times (Aqueous phase: [HCl]=4.0 mol/L, $[H_3PW_{12}O_{40}]$=30 g/L, and $[FeCl_3]$=20 g/L; Organic phase: 70 vol.% TBP, and T=(25±2) °C

The changes in the organic phase structure were investigated by FT-IR, and the results are shown in Fig. 11. Figure 11(a) shows the infrared absorption of a mixture composed of 70 vol.% TBP + 30 vol.% sulfonated kerosene. The absorption peak at 1281.9 cm^{-1} corresponded to the P═O bond vibration in alkyl phosphate [(RO)$_3$P═O]. The absorption peak at 1027.9 and 992.5 cm^{-1} corresponded to the P—O—C antisymmetric stretching vibration of the TBP molecule. Thus, the sulfonated kerosene in the organic phase did not alter the molecular characteristics of TBP. Figure 11(b) shows the infrared absorption spectra of the saturated loaded organic phase, which formed through the reaction between the organic phase and phosphotungstic acid solution. A strong wide spectrum band at 821.6 cm^{-1} corresponded to the stretching vibration of the O—W bond. The P═O

vibration absorption peak shifted to 1235.8 cm^{-1} owing to the formation of a stronger hydrogen bond [26]. This indicates a structural combination between the oxygen atom of the P═O group in TBP and the hydrogen atom of the phosphotungstic acid molecule. The formed hydrogen bond was considered as P═O·HO—P—W—O.

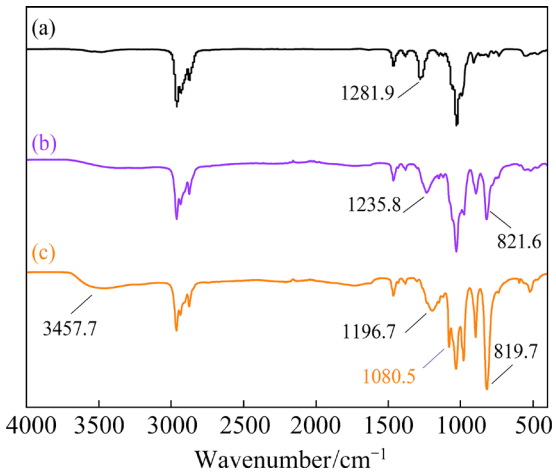

Fig. 11 FT-IR of organic phase: (a) 70 vol.% TBP+ 30 vol.% sulfonated kerosene; (b) $H_3PW_{12}O_{40}$ loaded organic (aqueous phase: [HCl]=4.0 mol/L, and [$H_3PW_{12}O_{40}$]= 30 g/L); (c) $H_3PW_{12}O_{40}$ + $FeCl_3$ loaded organic (aqueous phase: [HCl]=4.0 mol/L, [$H_3PW_{12}O_{40}$]=30 g/L, and [$FeCl_3$]= 20 g/L)

Figure 11(c) shows the infrared absorption spectra of the saturated loaded organic phase, which formed through the reaction between the organic phase and $FeCl_3$-containing phosphotungstic acid solution. The P═O stretching vibration absorption peak shifted to 1196.7 cm^{-1}, indicating the formation of a new hydrogen bond between TBP and the complex anion of iron. The spectra of Fe—O, TBP, and H_2O molecules exhibited stronger peaks at 1080.5 and 3457.7 cm^{-1}. Therefore, the form of $\left[H\cdot hH_2O\cdot qTBP\right]^{+}\left(FeCl_4\right)^{-}$ [30] can be presumed to represent the iron species in the organic phase. This structure confirms the salting-out effect produced by $FeCl_3$.

4 Conclusions

(1) The lg D of W and Fe was 2.51 and −0.34 at a TBP concentration of 0.5 mol/L, and the $\beta_{W/Fe}$ decreased with increasing TBP concentration. The extraction efficiency of W can be improved by increasing H^+ concentration of initial aqueous phase, and the Cl^- concentration only affects the extraction efficiency of Fe. The extraction efficiency of W was influenced by the $FeCl_3$ concentration in aqueous phase. As the initial $FeCl_3$ concentration increased from 20 to 50 g/L, the n value of TBP/$H_3PW_{12}O_{40}$ decreased from 0.89 to 0.72. TBP shows a higher tendency to bind with phosphotungstic acid when the organic phase approaches saturation-loading.

(2) The formation reaction of $H_3PW_{12}O_{40}\cdot nTBP$ is exothermic, and the structure of intermolecular hydrogen bond can be represented as P═O·HO—P—W—O. Fe(III) tends to form an extractive in the form of $\left[H\cdot hH_2O\cdot qTBP\right]^{+}\left(FeCl_4\right)^{-}$, and the salting-out effect enhances the extraction efficiency of W.

(3) This work illustrates that high acidity is beneficial for the exhaustive extraction of W, and points out that lower concentration of TBP and Cl^- are effective strategies for enhancing the separation of W to Fe.

CRediT authorship contribution statement

Li-qin DENG: Conceptualization, Methodology, Investigation, Data curation, Visualization, Writing − Original draft; **Xu-heng LIU:** Conceptualization, Methodology, Funding acquisition, Resources, Project administration, Supervision, Writing − Review & editing, Validation; **Xing-yu CHEN** and **Jiang-tao LI:** Investigation; **Li-hua HE:** Investigation, Funding acquisition; **Feng-long SUN:** Investigation; **Zhong-wei ZHAO:** Conceptualization, Funding acquisition, Project administration, Writing − Review & editing.

Declaration of competing interest

The authors declare that they have no known competing financial interests or personal relationships that could have appeared to influence the work reported in this paper.

Acknowledgments

This research was supported by the National key R&D Program of China (No. 2022YFC2905105), and the National Natural Science Foundation of China (No. 72088101).

References

[1] ZHAO Zhong-wei, SUN Feng-long, YANG Jin-hong, FANG Qi, JIANG Wen-wei, LIU Xu-heng, CHEN Xing-yu, LI Jiang-tao. Status and prospect for tungsten resources,

technologies and industrial development in China [J]. The Chinese Journal of Nonferrous Metals, 2019, 29(9): 1902−1916. (in Chinese)

[2] DAI Shu-gang, LI Jin-wang, WANG Chang-ji. Preparation and thermal conductivity of tungsten coated diamond/copper composites [J]. Transactions of Nonferrous Metals Society of China, 2022, 32(9): 2979−2992.

[3] YAN Nan-fu, CUI Hong-min, SHI Jin-song, YOU Sheng-yong, LIU Sheng. Recent progress of $W_{18}O_{49}$ nanowires for energy conversion and storage [J]. Tungsten, 2023, 5(4):371-390.

[4] WU Yong-lin, HONG Jia-bin, ZHONG Wei-xu, WANG Chun-xiang, LI Zhi-feng, SYDOROV Dmytro. Auxiliary ball milling to prepare WS_2/graphene nanosheets composite for lithium-ion battery anode materials [J]. Tungsten, 2024, 6(1): 124-133.

[5] WU Yu-han, XIA Wei-hao, LIU Yun-zhuo, WANG Peng-fei, ZHANG Yu-hang, HUANG Jin-ru, XU Yang, LI De-ping, CI Li-jie. Tungsten chalcogenides as anodes for potassium-ion batteries [J]. Tungsten, 2024, 6(2):278-292.

[6] SHEN Lei-ting, LI Xiao-bin, LINDBERG D, TASKINEN P. Tungsten extractive metallurgy: A review of processes and their challenges for sustainability [J]. Minerals Engineering, 2019, 142: 105934.

[7] YANG Xiao-sheng. Beneficiation studies of tungsten ores—A review [J]. Minerals Engineering, 2018, 125: 111−119.

[8] CHEN Chen, SUN Wei, ZHU Hai-ling, LIU Run-qin. A novel green depressant for flotation separation of scheelite from calcite [J]. Transactions of Nonferrous Metals Society of China, 2021, 31(8): 2493−2500.

[9] YANG Jin-hong, HE Li-hua, LIU Xu-heng, DING Wen-tao, SONG Yun-feng, ZHAO Zhong-wei. Comparative kinetic analysis of conventional and ultrasound-assisted leaching of scheelite by sodium carbonate [J]. Transactions of Nonferrous Metals Society of China, 2018, 28(4): 775−782.

[10] LEITÃO P, FUTURO A, VILA C, DINIS L, DANKD A, FIÚZA A. Direct pressure alkaline leaching of scheelite ores and concentrates [J]. Mining, Metallurgy & Exploration, 2019, 36: 993−1002.

[11] ZHAO Zhong-wei, LI Jiang-tao. Method for extracting tungsten from scheelite [P]. US20130195737, 2014.

[12] LEI Yun-tao, SUN Feng-long, LIU Xu-heng, ZHAO Zhong-wei. Understanding the wet decomposition processes of tungsten ore: Phase, thermodynamics and kinetics [J]. Hydrometallurgy, 2022, 213: 105928.

[13] LIAO Yu-long, ZHAO Zhong-wei. Effects of phosphoric acid and ageing time on solvent extraction behavior of phosphotungstic acid [J]. Hydrometallurgy, 2017, 169: 515−519.

[14] ZHU Ke-yu, REN Xiu-lian, LI Hua-quan, WEI Qi-feng. Simultaneous extraction of Ti(IV) and Fe(III) in HCl solution containing multiple metals and the mechanism research [J]. Separation and Purification Technology, 2021, 257(15): 117897.

[15] LI Yong-li, ZHAO Zhong-wei. Separation of molybdenum from acidic high-phosphorus tungsten solution by solvent extraction [J]. JOM, 2017, 69: 1920−1924.

[16] ASAKURA T, DONNET L, PICART S, ADNET J M. Extraction of hetero polyanions, $P_2W_{17}O_{61}^{10-}$, $P_2W_{18}O_{62}^{6-}$, $SiW_{11}O_{39}^{8-}$ by TBP [J]. Journal of Radioanalytical and Nuclear Chemistry, 2000, 246(3): 651−656.

[17] SMITH B J, PATRICK V A. Quantitative determination of aqueous dodecatungstophosphoric acid speciation by NMR spectroscopy [J]. Australian Journal of Chemistry, 2004, 57(3): 261−268.

[18] LIU W H, ETSCHMANN B, BRUGGER J, SPICCIA L, FORAN G, MCINNES B. UV−Vis spectrophotometric and XAFS studies of ferric chloride complexes in hyper-saline LiCl solutions at 25−90 °C [J]. Chemical Geology, 2006, 231(4): 326−349.

[19] CAI Xu-can, HAN Ji-xun, PANG Mao-ping, CUI Yu, LI Ye-xin, SUN Guo-xin. Structural effect of diamide extractants on the extraction behaviour of Fe(III) from hydrochloric acid [J]. Hydrometallurgy, 2016, 164: 48−53.

[20] HU Zhi-jin, ZHANG Tao, LV Li, CHEN Yan-xiao, ZHONG Ben-he, TANG Sheng-wei. Extraction performance and mechanism of TBP in the separation of Fe^{3+} from wet-processing phosphoric acid [J]. Separation and Purification Technology, 2021, 272(1): 118822.

[21] SHI Dong, CUI Bin, LI Li-juan, PENG Xiao-wu, ZHANG Li-cheng, ZHANG Yu-ze. Lithium extraction from low-grade salt lake brine with ultrahigh Mg/Li ratio using TBP−kerosene−$FeCl_3$ system [J]. Separation and Purification Technology, 2019, 211(18): 303−309.

[22] LUM K H, STEVENS G W, KENTISH S E. The modelling of water and hydrochloric acid extraction by tri-n-butyl phosphate [J]. Chemical Engineering Science, 2012, 84(24): 21−30.

[23] LEE H Y, KIM S G, OH J K. Stoichiometric relation for extraction of zirconium and hafnium from acidic chloride solutions with Versatic Acid 10 [J]. Hydrometallurgy, 2004, 73(1/2): 91−97.

[24] LEVITT A E, FREUND H. Solvent extraction of zirconium with tributyl phosphate[1] [J]. Journal of the American Chemical Society, 1956, 78(8): 1545−1549.

[25] KISLIK V S. Solvent extraction classical and novel approaches [M]. Amsterdam: Elsevier, 2012.

[26] AMARAL J C B S, MORAIS C A. Equilibrium of zirconium and hafnium in the process of extraction with TBP in nitric medium – Influence in the Zr/Hf separation [J]. Minerals Engineering, 2020, 146(15): 106138.

[27] LAKSHMANAN V I, HALDAR B C. Extractive behavior of 12-heteropoly acids. I. Extraction of 12-tungstophosphoric acid [J]. Journal of the Indian Chemical Society, 1969, 46(6): 512−524.

[28] LAKSHMANAN V I, HALDAR B C. Extractive behavior of 12-heteropoly acids. III. Extraction of 12-tungstophosphoric, 12-molybdophosphoric, 12-tungstosilicic, and 12-molybdosilicic acids by TBP in organic diluents [J]. Journal of the Indian Chemical Society, 1970, 47(1): 72−78.

[29] ZHANG Shao-jie, CHEN Yan-xiao, ZHANG Tao, LV Li, ZHENG Dong-yao, ZHONG Ben-he, TANG Sheng-wei. Separation of H_3PO_4 from HCl-wet-processing phosphate rocks leach liquor by TBP: Extraction equilibria and mechanism study [J]. Separation and Purification Technology, 2020, 249(15): 117156.

[30] MA Rong-jun. Extractive metallurgy [M]. Beijing: Metallurgical Industry Press, 2009. (in Chinese)

TBP−HCl−H_2O 萃取体系中钨和铁的竞争行为

邓立勤[1]，刘旭恒[1]，陈星宇[1]，李江涛[1,2]，何利华[1]，孙丰龙[1,2]，赵中伟[1,2]

1. 中南大学 冶金与环境学院，长沙 410083；
2. 中南大学 稀有金属冶金与材料制备湖南省重点实验室，长沙 410083

摘　要：通过调控萃取剂浓度和溶液环境研究磷钨酸和氯化铁在 TBP−HCl−H_2O 体系中的分布和竞争行为。结果表明，随着 TBP 浓度的降低，TBP 对磷钨酸的亲和力更强。在高酸度条件下 W 的萃取效率更高，而降低水相 Cl^- 浓度会抑制 TBP 对 Fe 的萃取。当有机相接近饱和负载时，磷钨酸能够竞争性地取代铁与 TBP 分子结合。FT-IR 表征阐明了磷钨酸和 TBP 之间的氢键结合形式(P═O·HO—P—W—O)，解释了 $FeCl_3$ 诱导的盐析效应。因此，提高酸度有利于钨的深度萃取，而降低 TBP 和 Cl^- 浓度是实现 W/Fe 分离的有效措施。

关键词：溶剂萃取；磷酸三丁酯；钨/铁分离；分布平衡；竞争行为

(Edited by Xiang-qun LI)